

PROFILE MEASUREMENT OF HIGH ASPECT RATIO MICRO STRUCTURES USING A TUNGSTEN CARBIDE MICRO CANTILEVER COATED WITH PZT THIN FILMS

Masaki Yamamoto*, Isaku Kanno**, and Shinichiro Aoki*

* Opto-Electro Mechanics Research Laboratory, Matsushita Research Institute Tokyo, Inc.
3-10-1 Higashimita, Tama-ku, Kawasaki 214-8501, Japan

** Human Environmental Systems Development Center, Matsushita Electric Industrial Co., Ltd.

ABSTRACT

A new profile measurement probe for non-destructive evaluation of high aspect ratio micro structure (HARMS) is proposed. The probe is made of tungsten carbide super hard alloy (WC) and machined by micro EDM. PZT thin films are coated on the probe as an integrated strain sensor. Dedicated measurement machine equipped with this probe is developed and we observed micro holes and gears. In these observations, we obtained very clear images of the sample's detailed shapes, which demonstrate the system's validation for HARMS evaluation.

INTRODUCTION

Recent development in the field of high aspect ratio micro structure technologies (HARMST) accelerates the need for nondestructive measurement of such structures. For example, contemporary micro nozzle tests have been done by actually spraying liquid from the holes. The drawback; the test fails to give the exact location of the defect, thus stirring a desire for the measurement of hole profile and internal surface roughness. In the micromachine field, micro gears by EDM and LIGA are beginning to be used in practice. The evaluation of tooth surface roughness and wear of such gears call for a new measurement method.

HARMS measurement has inherent difficulties because high walls stand with extremely narrow spacing for probing means. Because the vertical surface doesn't reflect light back, optical methods are not suitable for three-dimensional evaluation. Thus, measurement with physical contact probes seems to be the promising solution for HARMS nondestructive evaluation.

The first approach for HARMS measurement is conventional mechanical probing measurement such as coordinate measurement machine (CMM). The smallest probe readily available as of present is $\phi 0.2$ mm. Because the probing force decides the minimum probe size, low contact force systems have been investigated (for example, [1,2]). Although these approaches have succeeded in realizing $1\mu\text{N}$ probing force and $\phi 100$ micron fiber probes respectively, the difficulty of probe assembly limits further downsizing of the CMM probe. Another promising approach for HARMS measurement

is the AFM. Because most AFM systems are designed for planer samples like Si wafers, they employ a light leverage method to detect the probe's strain. As a result, when the probe is inserted into microstructures, the detective light can easily be obstructed and the system fails. One exception is critical dimension AFM (CD-AFM) [3]. Equipped with a flare-shape tip, this device can measure a trench of maximum $8\mu\text{m}$ depth and minimum $0.5\mu\text{m}$ width, which is used for device isolation in LSI process. Thanks to the recent progress in AFM probe technology, AFM probes can have their own integrated strain sensor (for example, [4]). These probes can be vertically inserted into micro holes and can measure the surface, once the measurement setup is prepared. Although the AFM approach seems to be a good candidate for HARMS measurement, its rigid probe dimension can be an obstacle. In other words, requirements for probe dimension can change according to the measurement sample because the probe and its tip dimension decide the maximum depth, maximum protrusion and minimum gap it can handle. Lithographically manufactured AFM probes cannot change shape once the mask pattern and the process conditions are fixed.

Vibrosensing Method

The third approach for HARMS measurement is to utilize a flexible manufacturing technology for custom-made probes. Such an example is the vibrosensing (VS) method [5] that uses a probe machined by WEDG technology [6]. WEDG is a variation of EDM and works as a NC lathe for micro parts such as pins or cones. The probe is vibrated at a low frequency, 100Hz,

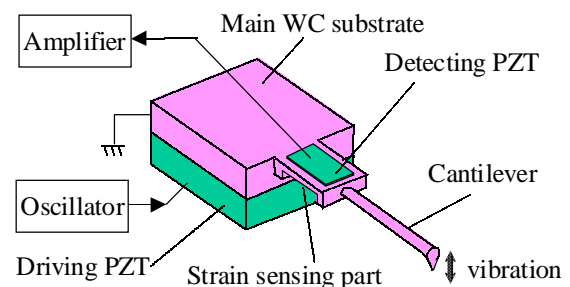


Figure 1: Structure of RVS probe.

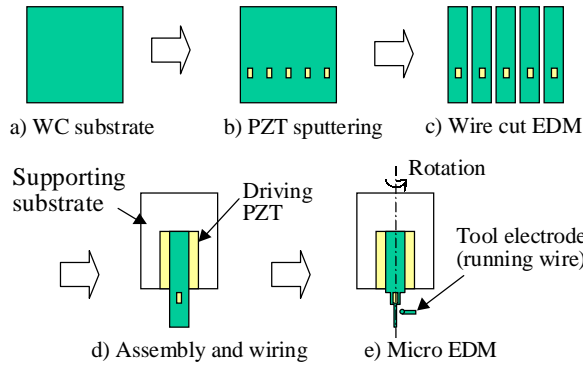


Figure 2: Fabrication process of RVS probe.

with amplitude of 2 μm , and detects the surface by electric conductivity. From its principle, the VS method cannot be applied to nonconductive samples or thick oxide layers. Nevertheless, the VS method is confirmed to be a robust measurement tool for on-the-machine evaluation of micro EDMed sample [7]. To overcome the shortcoming of the VS method, the twin probe vibroscanning method was proposed [8]. By utilizing the twin cantilever and detecting the conductivity between them, contact to the surface can be detected irrespective to the sample's electric conductivity. Drawbacks which still remain include the fact that the electric contacts are open to the air and vulnerable to dust and oxidation. Moreover, the total thickness of the probe cannot be minimized, as it requires two cantilevers.

Based on the above-mentioned survey, we have concluded that a combination of AFM technology and VS technology gives the best methodology for HARMS measurement [9]. In other words, the new probe should accompany an AFM-like integrated strain sensor while maintaining VS's flexible probe shape control. In this report, we describe the new method with emphasis on the latest development with PZT thin films.

A NEW MEASUREMENT PROBE

In a new probe, the key is how to form a strain sensor on a cylindrical cantilever machined by WEDG. Our solution is to divide the cantilever and strain sensing part as shown in Figure 1. The main WC substrate is made of tungsten carbide super hard alloy, which is a popular material as a mechanical probe for its high hardness and Young's modulus. The WC main plate is machined into a thin round cantilever, which is vibrated at its resonance by the driving PZT. The vibration is detected by the PZT thin film formed on the thinned stress sensing part which is also machined by WEDG. The contact of the probe to the sample surface can be detected by the change of the vibration amplitude. We call the technology "resonance mode vibroscanning

method" (RVS) with respect to the fact that it employs the same cantilever technology as in VS.

RVS Probe Fabrication

Figure 2 shows the probe's fabrication process. On a lapped WC substrate, patterned PZT thin films of 2.5 μm thickness are deposited with top and bottom Pt-electrodes by the method stated below. In (c), the substrate is separated by wire cut EDM into individual pieces. The WC piece is assembled on a supporting substrate with a driving PZT and necessary wiring is done in (d). The assembled body is then mounted on NC controlled micro EDM (Matsushita MG-ED72) and the cantilever and strain sensing part are machined. Forming the cantilever after cartridge assembly enables it to be accurately aligned to the cartridge, thus guaranteeing high mounting accuracy on the measurement machine. The total fabrication process is the most favorable combination of AFM-like (batch) and VS-like (piecewise) process. In the process from (a) through (c), batch process is employed for mass production. On the contrary, in the process of (d) and (e), piecewise process is employed to maximize design freedom. In other words, each manufactured probe cartridge can have a custom-made probe shape for each application thanks to WEDG's NC machining.

PZT Thin Films

PZT films were deposited using rf-magnetron sputtering technique. Substrates used were WC, coated with (111)-oriented Pt (300 nm)/Ti (30 nm) layers. In order to obtain PZT films with a stable composition near the morphotropic phase boundary, a ceramic PZT target with a composition of $[\text{Pb}(\text{Zr}_{0.53}\text{Ti}_{0.47})\text{O}_3 + 20\text{mol}\%\text{PbO}]$ was sputtered. It was confirmed that the composition of the resulting films is almost same as that of target by the compositional measurements with an energy-dispersive x-ray microanalyzer [10]. PZT films were grown in at a substrate temperature about 600 $^{\circ}\text{C}$ until the thickness of the films were about 2.5 μm with a

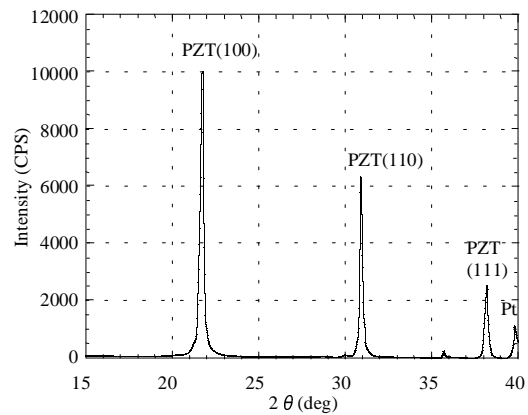


Figure 3: XRD pattern of PZT films deposited on WC substrate.

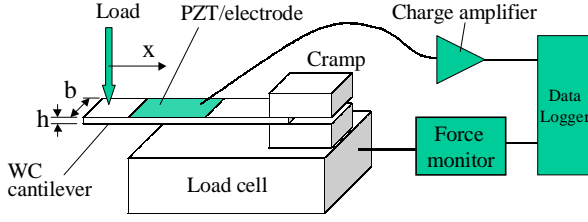


Figure 4: Measurement of piezoelectric coefficient d_{31} .

high deposition rate about 1 $\mu\text{m}/\text{h}$. Crystalline structure of the prepared PZT films was examined by x-ray diffraction (XRD) measurement. Figure 3 shows the XRD pattern of the PZT film. It revealed that the PZT films were successfully grown with perovskite structure on the Pt-coated WC substrates.

Piezoelectric properties of the resulting PZT films were observed by measuring the piezoelectric charge from the external stress on the films. In the previous study, we have confirmed the sputtered PZT films were naturally and stably polarized from the bottom to the surface of the films [11]. Therefore we carried out the piezoelectric measurement for the as-deposited films without any poling treatments. It is to be noted that these polarization properties are very suitable for device application using piezoelectric thin films. A schematic configuration of the measurements is given in Figure 4. We deposited Pt top electrode on the PZT films and detected piezoelectric charge using the charge amplifier, applying load on the edge of the sample. When the load (W) is applied, the stress (σ_{PZT}) of the PZT film is expressed as follows, with the assumption that the film is thin enough compared to the substrate:

$$\sigma_{\text{PZT}} \cong \frac{E_p M}{E_s I_s} \cdot y = \frac{E_p W x}{E_s \frac{bh^3}{12}} \cdot \frac{h}{2}$$

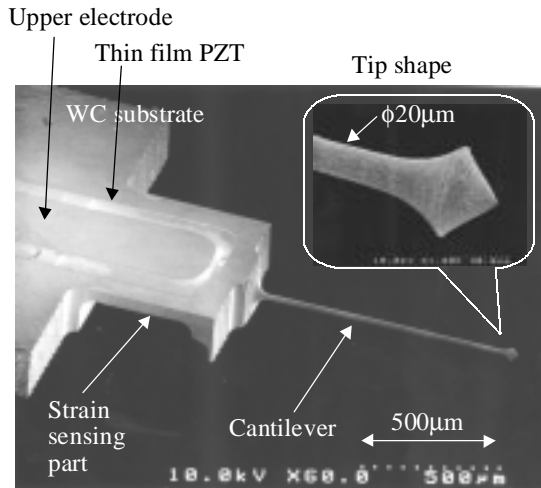


Figure 5: SEM micrograph of RVS probe.

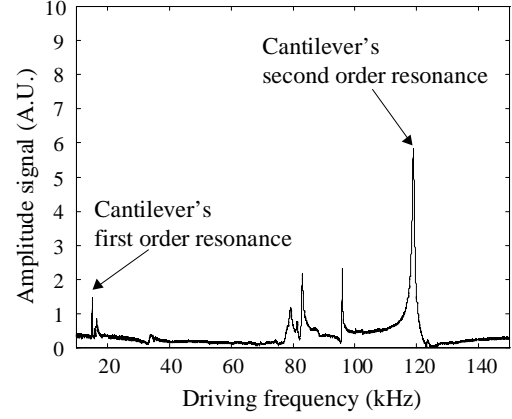


Figure 6: Frequency response of RVS probe.

where E_p and E_s are the Young's modulus of the PZT and WC, M is the moment, b is the width of the sample, h is the thickness of the WC substrate, x is the distance from the load point to the electrode. Piezoelectric constant d_{31} is formulated as:

$$d_{31} = \frac{Q}{\int_S \sigma_{\text{PZT}} dS}$$

where Q is the piezoelectric charge, and S is the area of the Pt top electrode. With the values of $E_p = 63 \text{ GPa}$ [12] and $E_s = 560 \text{ GPa}$, we have obtained the PZT's piezoelectric constant $d_{31} = 85 \text{ pC/N}$. This value is comparable to bulk material's piezoelectric constant.

RVS Probe Evaluation

Figure 5 is a SEM micrograph of the RVS probe. The cantilever is a cylindrical rod to cancel machining stress. Tip shape can be like AFM tip (L shape) with additional EDM machining. The L shaped tip is used for further downsizing the probe size. Figure 6 is the probe's frequency response in which the cantilever's first and second resonance is clearly observed at 15 kHz ($Q=400$) and 119 kHz ($Q=100$). Although there is a lump at the

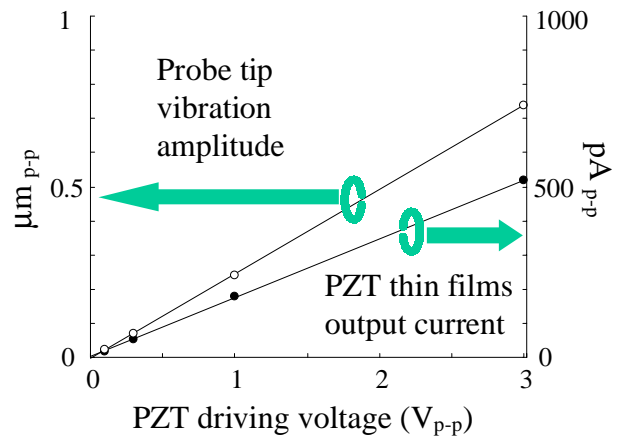


Figure 7: Probe amplitude vs. PZT driving voltage

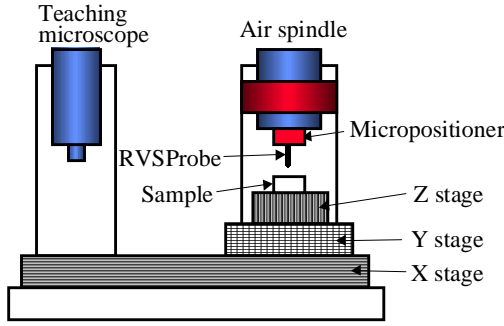


Figure 8: Configuration of measurement machine.

probe tip, the resonance frequency can be approximated using a vibrating cantilever's equation [13]. The calculated values were 20 kHz and 125 kHz for the probe, which corresponds well with the experimental values. In the contact detection, the second mode resonance is used based on the fact that the lower Q and larger signal output can realize faster response and high S/N in the contact detection, respectively.

In Figure 7, the tip amplitude is experimentally measured by laser doppler velocity meter. Oscillating piezoelectric charge is monitored as a piezoelectric current by the charge amplifier. The second mode resonance is used for the measurement. Tip amplitude was $0.24 \mu\text{m}_{\text{p-p}}$ and piezoelectric current was $180 \text{ pA}_{\text{p-p}}$ for $1 \text{ V}_{\text{p-p}}$ PZT driving voltage. Both amplitude and piezoelectric current are perfectly proportional to the PZT driving voltage. Using this relationship, the amplitude is set to $0.1 \mu\text{m}_{\text{p-p}}$ in the following measurement experiments.

MEASUREMENT MACHINE

In conventional CMM, the measurement probe can easily be observed by the naked eye. In HARMS measurement, on the other hand, even inserting the probe into the region of interest is a painful process. To

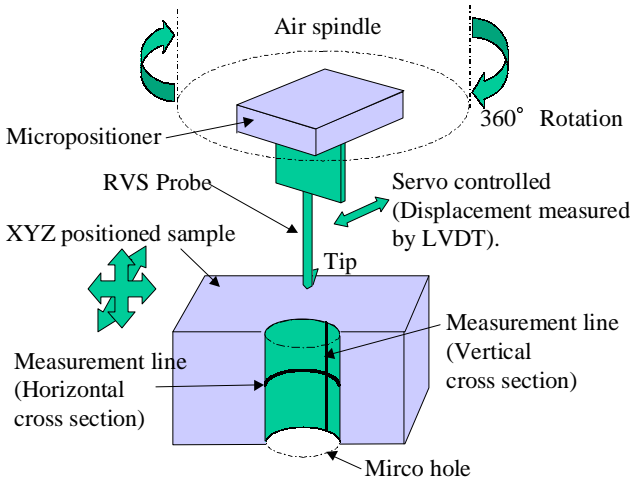


Figure 9: Micro hole cross section measurement.

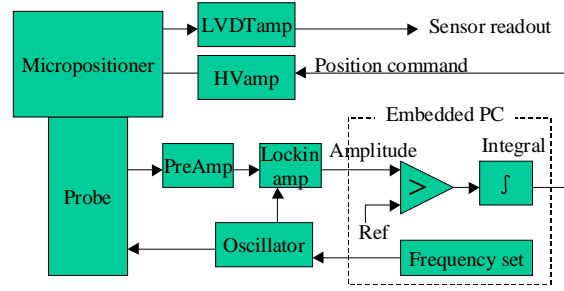


Figure 10: Block diagram of the control system

handle HARMS's specific difficulties, we have also developed a dedicated measurement machine.

As in Figure 8, the measurement system has a teaching microscope, measurement probe, and XYZ stage. As the positional relationship between the microscope focal point and probe tip is fixed, once an operator instructs points in the microscope image, the probe can be automatically inserted into the sample and perform the measurement automatically. The sample is positioned by an XYZ air slide system. The XY air slides are actuated by two linear motors with feedback of a 10nm resolution linear scale. The Z stage is guided by air slide and driven by ball screw. The Z stage position is monitored by a 20nm linear scale but employs no feedback control. The smooth motion of the air slide guarantees submicron measurement accuracy. The micropositioner, under which the probe is vertically held as shown in Figure 9, consists of a PZT actuator, displacement amplifying mechanism and a LVDT sensor. The total travel of the micropositioner is $100 \mu\text{m}$. By the micropositioner, the tip contact condition is kept constant. Since the micropositioner's displacement is limited to one direction, a rotary air spindle with an accuracy of over $0.1 \mu\text{m}$ is equipped. Using the operator's registered instructions, the spindle rotates the micropositioner so that the probe tip faces the measurement surface at the right angle.

Figure 10 is the block diagram of the control system. The embedded PC, which reads the probe's amplitude,

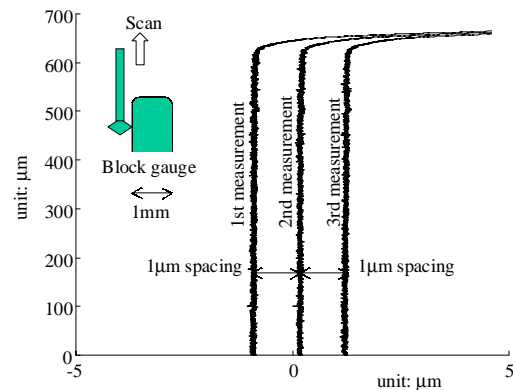


Figure 11: Measurement resolution and repeatability

controls the micropositioner's position in an integral manner through the high voltage (HV) amplifier. The control interval is 2 mS which is limited by the micropositioner's response time. The step size used in the positional integration is 0.1 μm . The probe's accurate position is always monitored by LVDT. The lockin amplifier is used to enhance the S/N of the probe's signal even when the tip amplitude is set to less than 0.1 μm .

MEASUREMENT EXPERIMENTS

Figure 11 is repetitive measurements of block gauge surface to examine the resolution and the repeatability. The probe scans vertically up along the gauge surface for three times. The measurement results are drawn with 1 μm horizontal separation, which shows good coincidence to the level of 0.1 μm . As the servo control's resolution is 0.1 μm , the RVS probe's inherent resolution can be said to be better than 0.1 μm . As for the repeatability, there are slight differences in the three measurements, which we attribute to dusts or other small contamination on the gauge surface.

Figure 12 and 13 are the results of sample measurements. In Figure 12, a double-side etched hole in the 200 μm thick stainless steel is nondestructively examined. An optical microscope image and a vertical cross section are shown in the upper left and right hand corners respectively. The center image is a three dimensional display of the hole's inner surface. The measurement was done by consecutive cross-sectioning at 3 μm interval and all cross sections are smoothly reconstructed in three-dimensional space later. Figure 13 is a micro gear, which is machined by micro EDM with intentionally wrong machining parameters. In Figure 13(a), the gear's module is 29 μm and the narrowest gap between the teeth is 40 μm . The circled tooth is cross-sectioned at 3 μm interval. The surface profile (c) shows surface roughness due to the course machining condition, and vertical traces caused by

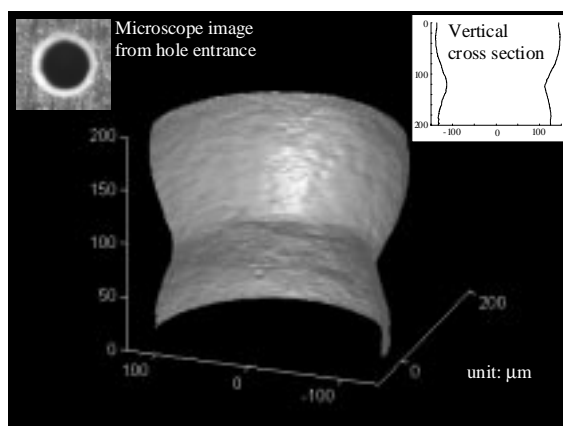


Figure 12: Three dimensional rendering of etched micro hole.

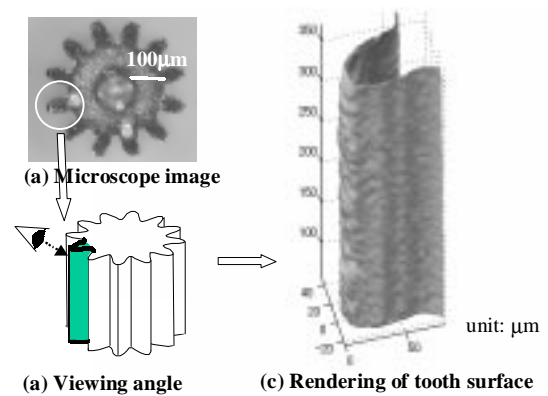


Figure 13: Three dimensional rendering of a micro gear tooth.

EDM electrode's trajectory.

DISCUSSION

Figure 14 shows several variations of the probe tip. Probe (a) is an L shaped probe. In the photo, the axis is $\phi 40 \mu\text{m}$ and tip length is 40 μm . Long tip length is useful to scan overhung structures, such as a reverse tapered hole or through-hole bottom edge. Probe (b) is a ball shaped probe, which is an analogy from a CMM probe. Probe (c) is an ultra high aspect ratio probe, $\phi 12 \mu\text{m}$ in diameter and 1000 μm in length. The minimum possible diameter as of present is 10 μm , attempts for smaller diameter resulted in the bend of the probe caused by residual stress.

RVS application for HARMS measurement is basically limited by the available probe shape. Figure 15 is a rough sketch of the RVS application area, taking micro holes as examples. In the chart, CD-AFM and CMM application areas are also drawn for comparison. The area of RVS ranges from 20 to 500 μm in diameter and 10 – 2000 μm in depth. The smallest diameter is defined by the thinnest possible probe, and the maximum comes from the competition with CMM. The maximum depth is decided by the WC substrate size we prepare. As we

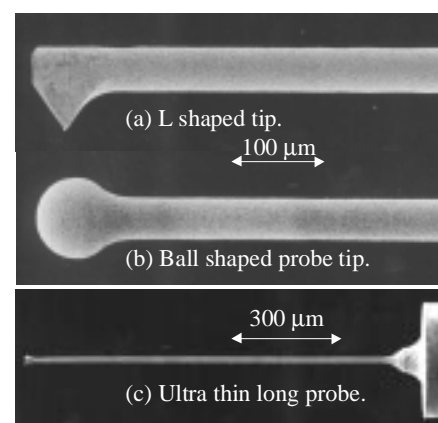


Figure 14: RVS probe shape variations

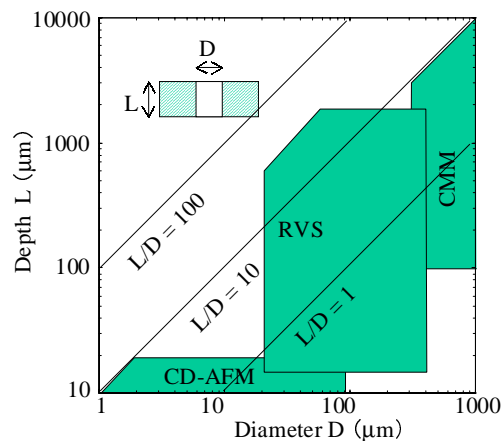


Figure 15: RVS Application area in HARMS measurement

limit the cantilever's aspect ratio to less than 100, the maximum aspect ratio of the hole should be less than 30. As is clear from the chart, the RVS method fills the vacancy between CD-AFM and CMM.

One drawback of the RVS probe is its relatively uncertain tip radius. Because EDM uses electro discharge heat to remove material, EDM craters on the workpiece are inevitable. The tip curvature radius is directly affected by the craters, and varies from 0.5 to 2 μm in our SEM observations. In order to make the tip shape constant, we are now preparing a debarring process for the tips.

CONCLUSION

Based on a survey of the current technologies for HARMS measurement, we have proposed a new approach: the resonance mode vibroscanning method (RVS). The RVS probe inherits favorable characteristics of both VS and AFM methods. It is made of tungsten carbide super hard alloy and has flexibility in its shape and size (VS properties). It also has an integrated strain sensor to detect contact at a low contact force (AFM properties). PZT thin films is successfully deposited on the WC substrate and its high performance is confirmed both in dielectric constant measurement and in its real application as the strain sensor. The probe is attached to a newly proposed HARMS dimensional measurement machine. The resolution of the probe is confirmed to be better than 0.1 μm . The internal profile and roughness of a chemically etched hole and EDMed micro gear were examined. These results illustrate the validity of RVS for its intended application as a method for HARMS measurement.

ACKNOWLEDGEMENT

A part of this work was performed under the management of the Micromachine Center as the

Industrial Science and Technology Frontier Program, "Research and Development of Micromachine Technology", of MITI supported by the New Energy and Industrial Technology Development Organization. The authors gratefully acknowledge suggestions and encouragement by Prof. Masuzawa of the University of Tokyo.

REFERENCES

- [1] W.O. Pril, et al., "Development of a 2D probing system with nanometer resolution," American Soc. Prec. Eng. 16, pp. 438-442, 1997.
- [2] K. Schepperie, et al., "Coordinate measuring apparatus having a probe in the form of a solid-state oscillator," USP5782004, 1998.
- [3] G. Vachet and M. Young, "Critical dimension atomic force microscopy for 0.25-micrometer process development," Solid State Technology 38, pp. 57-62, 1995.
- [4] P.F. Indermuhle, et al. "Atomic force microscopy using cantilevers with integrated tips and piezoelectric layers for actuation and detection," J. Micromech. Microeng. 7, pp. 218-220, 1997.
- [5] T. Masuzawa, et al., "Vibroscanning method for nonde-structive measurement of small holes," Annals of the CIRP, 42, pp. 589-592, 1993.
- [6] T. Masaki, et al. , "Micro electro-discharge machining and its applications," Proc. IEEE MEMS, pp. 21-26, 1990.
- [7] M. Yamamoto, et al., "Application of vibroscanning method to on-the-machine measurement of micro electro discharge machining," Int. J. Japan Soc. Prec. Eng. 30, pp. 49-50, 1996.
- [8] T. Masuzawa, et al., "Twin-probe vibroscanning method for dimensional measurement of microholes," Annals of the CIRP 46, pp. 437-440, 1997.
- [9] M. Yamamoto, et al., "Dimensional Measurement of High Aspect Ratio Micro Structures with a Resonating Micro Cantilever Probe," HARMST '99, pp. 56-57, 1999.
- [10] I. Kanno, et al., "Piezoelectric properties of c-axis oriented Pb(Zr,Ti)O₃ thin films," Appl. Phys. Lett., 70 (11), pp. 1378-1380, 1997.
- [11] J. F. Shepard, et al, "Characterization and aging response of the d₃₁ piezoelectric coefficient of lead zirconate titanate thin films," J. Appl. Phys. 85, pp. 6711-6716, 1999.
- [12] T.S. Low and W. Guo, "Modeling of a Three-Layer Piezoelectric Bimorph Beam with Hysteresis," J. MEMS 4, pp. 230-237, 1995.
- [13] D. Sarid, "Scanning Force Microscopy," Oxford University Press, Chapter 1, 1994.

